

Spin canting phenomenon in cadmium doped cobalt ferrites, $\text{CoCd}_x\text{Fe}_{2-x}\text{O}_4$ ($x = 0.0, 0.2, 0.4, 0.6, 0.8$ and 1.0), synthesized using sol–gel auto combustion method

SONAL SINGHAL*, SHEENU JAUHAR, KAILASH CHANDRA† and SANDEEP BANSAL‡

Department of Chemistry, Panjab University, Chandigarh 160 014, India

†33/1, Bhagirath Kunj, Railway Station Road, Roorkee 247 667, India

‡Department of Science and Technology, New Delhi 110 016, India

MS received 23 November 2011; revised 19 April 2012

Abstract. Synthesis of non-collinear (spin canted) ferrites having the formula, $\text{CoCd}_x\text{Fe}_{2-x}\text{O}_4$ ($x = 0.0, 0.2, 0.4, 0.6, 0.8$ and 1.0), has been carried out using the sol–gel auto combustion method. The ferrite samples show an interesting magnetic transition from Neel to Yafet–Kittel configuration, as the Cd^{2+} concentration is increased beyond $x = 0.4$. The FT–IR spectra confirm the formation of the metal oxide bond as they exhibit two frequency bands in the range of $\sim 595\text{ cm}^{-1}$ and $\sim 450\text{ cm}^{-1}$, corresponding to the tetrahedral and the octahedral stretching vibrations of the metal oxide, respectively. The structural evolutions of the nanophase investigated using powder X-ray diffraction (XRD) technique show that the average crystallite size is $\sim 35\text{ nm}$. The magnetic studies reveal that the saturation magnetization, M_s , increases up to $x = 0.4$ and decreases when the value of x is >0.4 . It is proposed that the incorporation of Cd^{2+} ion takes place into the tetrahedral sites and up to $x = 0.4$, Neel’s model is followed. But for $x > 0.4$, canting of spins occurs, as explained by Yafet–Kittel (Y–K) model. The d.c. resistivity decreases as a function of temperature, indicating semiconducting nature of the ferrites and the positive value of Seebeck coefficient establishes p -type conduction behaviour for all the ferrite samples.

Keywords. Transmission electron microscope; electrical resistivity; spin canting.

1. Introduction

The ferrimagnetic structures having canted or non-collinear spins are a subject of considerable interest because of their versatile properties and potential applications in electronics, optical devices, magnetic storage devices, coolants, sensors, multi-layer chip inductors and health and medicine e.g. magnetically guided drug delivery and magnetic resonance imaging (MRI) contrast agent (Rai *et al* 2011; Shelar *et al* 2009). They also find extensive applications as permanent magnets in microwave devices, television sets, bubble devices of computer and as inductor surface mount devices in electronic products such as cellular phones, digital diaries and video cameras. Such ferrites have been regarded as better magnetic materials than pure metals because of their high resistivity, higher efficiency and low cost (Deraz and Hessian 2009).

The spin canting phenomenon has been commonly observed in diamagnetically substituted spinel ferrites, having the general formula $M\text{Fe}_2\text{O}_4$ (where M is a divalent cation). These have been extensively studied due to their unique electrical and magnetic properties, high resistivity, mechanical hardness and chemical stability. The diversity in the properties of such ferrites arises due to the fact that

the spin canting depends on composition, temperature and applied magnetic fields. Further, a variety of transition metal cations can be incorporated into the lattice of the parent magnetic structure and these cations alter their properties by affecting the distribution of the cations among the tetrahedral (A) and the octahedral (B) sites. The first attempt to explain spin canting in ferrites was made by Yafet and Kittel (1952). They considered that a ferrimagnet with two crystallographic sublattices, A and B, have antiferromagnetic A–A, B–B and A–B exchange couplings. It is also assumed that B sublattice splits in the B_1 and B_2 sublattices, having equal magnetic moments, each making an angle α_{YK} with the direction of the net magnetization at 0 K. $2\alpha_{YK}$ is the angle between the moments on the B_1 and B_2 sites. The resultant moment of the B sublattice is antiparallel but collinear to that of the A-sublattice.

It is well known that cadmium substitution modifies the magnetic and electrical properties of the ferrites to a considerable extent. The electronic configuration of Cd^{2+} ion with free $5s$ and $5p$ orbitals permit it to form covalent bonds with oxygen ions and predispose them to occupy tetrahedral sites only (Prasad *et al* 2011). Due to the immense importance of cadmium substituted ferrites, numerous studies have been conducted to study the spin canting phenomenon in such ferrites (Abdeen *et al* 2002; Ravinder *et al* 2003; Shelar *et al* 2009; Akhter and Hakim 2010;

*Author for correspondence (sonal1174@gmail.com)

Chandradass *et al* 2010; Anjum *et al* 2011). Various preparation techniques like sol–gel method, co-precipitation method, ball milling, microemulsion processing, etc have been developed in order to obtain cadmium substituted ferrites with tunable physical properties. Many research groups are working on optimizing the magnetic and electrical properties of such ferrites by varying parameters such as temperature, pH, complexing agent, etc. Shelar *et al* (2010) reported the synthesis of nickel cadmium ferrites, $\text{Ni}_{1-x}\text{Cd}_x\text{Fe}_2\text{O}_4$, using self propagating combustion method and observed that the increase in cadmium concentration expands the lattice parameter, in accordance with Vegard's law. The saturation magnetization increases as the Cd content is increased. Abdeen *et al* (2002) employed ceramic technique to synthesize cadmium substituted cobalt ferrites, $\text{Co}_{1-x}\text{Cd}_x\text{Fe}_2\text{O}_4$. Their d.c. electrical conductivity increased with increasing temperature and increasing cadmium content. The ferrites show maximum d.c. conductivity at $x = 0.7$, at which the activation energy for conduction becomes minimum. Further, the increase in Cd content leads to increase in the transition temperature, T_c . Akhter and Hakim (2010) reported that the magnetic moment and the saturation magnetization of cadmium substituted lithium ferrites, $\text{Li}_{0.5-x/2}\text{Cd}_x\text{Bi}_{0.02}\text{Fe}_{2.48-x/2}\text{O}_4$, increase up to $x = 0.3$ and then decrease for $x > 0.3$, arising due to the formation of spin canted structures. Similar results have been obtained by Anjum *et al* (2011), who studied the structural and magnetic properties of cadmium substituted nickel aluminum ferrites, $\text{Ni}_{1-x}\text{Cd}_x\text{Al}_{0.6}\text{Fe}_{1.4}\text{O}_4$. They reported that the saturation magnetization increases up to $x = 0.5$ and then decreases as the value of x is increased to 0.75. Ravinder *et al* (2003) calculated the negative values for Seebeck coefficients of cadmium substituted nickel ferrites, indicating that they behave as n -type semiconductors.

In view of the distinctive influence of cadmium substitution in ferrites, it is considered necessary to systematically study the effect of incorporation of Cd^{2+} ions in cobalt ferrites. Therefore, the present work deals with the synthesis of cadmium substituted cobalt ferrites via sol–gel auto-combustion method. The authors also investigate the effect of Cd^{2+} ions on the structural, magnetic and electrical properties of substituted cobalt ferrites.

2. Experimental

Magnetic nanoferrites with chemical formula, $\text{CoCd}_x\text{Fe}_{2-x}\text{O}_4$ ($x = 0.0, 0.2, 0.4, 0.6, 0.8$ and 1.0), have been synthesized using sol–gel auto combustion method because of the low processing temperature, good stoichiometric control, homogenous distribution of reactants and production of ultra fine particles with narrow size distribution. To prepare these ferrites, stoichiometric amounts of $\text{Fe}(\text{NO}_3)_3 \cdot 9\text{H}_2\text{O}$ (Merck), $\text{Co}(\text{NO}_3)_2 \cdot 5\text{H}_2\text{O}$ (s.d. fine-chem limited), $\text{Cd}(\text{NO}_3)_2 \cdot 4\text{H}_2\text{O}$ (Qualigens) and citric acid (weighed as citric acid/metal ion mole ratio of 1:1) were weighed and dissolved separately in minimum amount of distilled water. The individual

solutions were then mixed and pH of the resulting solution was adjusted to 5–6 by adding dilute ammonia solution. The solution was then stirred on a hot plate magnetic stirrer till the gels were formed which were then ignited in a self-propagating combustion manner to yield nanoferrite particles. The ferrite samples were then annealed at various temperatures of 400 °C, 600 °C, 800 °C and 1000 °C for 2 h in a muffle furnace (Chandradass *et al* 2010).

The FT–IR spectra for all the samples have been recorded by Perkin–Elmer RX-1 FT–IR spectrophotometer with KBr pellets in the range 4000–400 cm^{-1} . Powder X-ray diffraction (XRD) patterns have been recorded using a panalytical's X'pert pro spectrophotometer with Cu-K α radiation. Hitachi (H-7500) TEM operated at 120 kV has been used to record micrographs of the synthesized samples. The magnetic properties have been measured using a vibrating sample magnetometer (VSM) (155, PAR). The electrical properties have been studied using a two-probe method.

3. Results and discussion

3.1 FT–IR characterization

The infrared spectrum is of great importance as it is sensitive to the short range environment of the oxygen coordination around the cations in both tetrahedral and octahedral clusters of the ferrites. The spectra of all the ferrites have been recorded in Nujol using KBr plates. The FT–IR spectra of all the samples annealed at 400, 600 and 1000 °C exhibit two main absorption bands below 1000 cm^{-1} , corresponding to the vibrational modes of all the spinel compounds, confirming the formation of the metal oxides. The occurrence of the band in the range of $\sim 595 \text{ cm}^{-1}$ has been assigned to the intrinsic vibrations of the tetrahedral complexes corresponding to the highest restoring force, whereas that in the range of 445–465 cm^{-1} is attributed to the intrinsic vibrations of the octahedral complexes, which are bond bending vibrations (Waldron 1955; Cedeño-Mattei and Perales-Pérez 2009). Therefore, vibrational mode of tetrahedral clusters is higher than that of octahedral mode (Shelar *et al* 2009). It is observed that the band in the range of 445–465 cm^{-1} is broad. Similar results have also been reported by Cedeño-Mattei and Perales-Pérez (2009), who have suggested that the broad peak may have resulted from a poor development of crystallinity in the ferrite samples. A sharp peak at 720 cm^{-1} is given by nujol. FT–IR spectra of all the ferrites annealed at 1000 °C are shown in figure 1.

3.2 Transmission electron microscopy (TEM) studies

TEM images of all the ferrite samples annealed at 1000 °C have been recorded by ultrasonically agitating the ferrite samples. Figure 2 shows typical TEM micrograph of $\text{CoCd}_{0.2}\text{Fe}_{1.8}\text{O}_4$ annealed at 1000 °C. It can be seen from the figure that there is a formation of highly agglomerated particles. The agglomeration of the particles might have

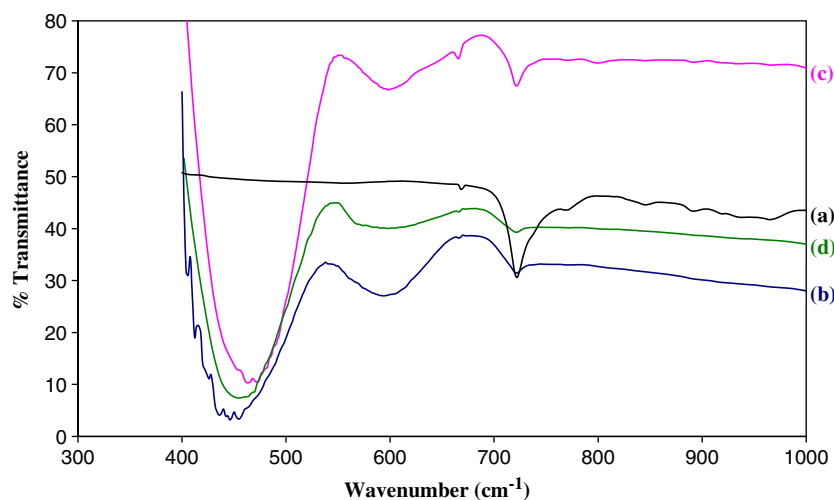
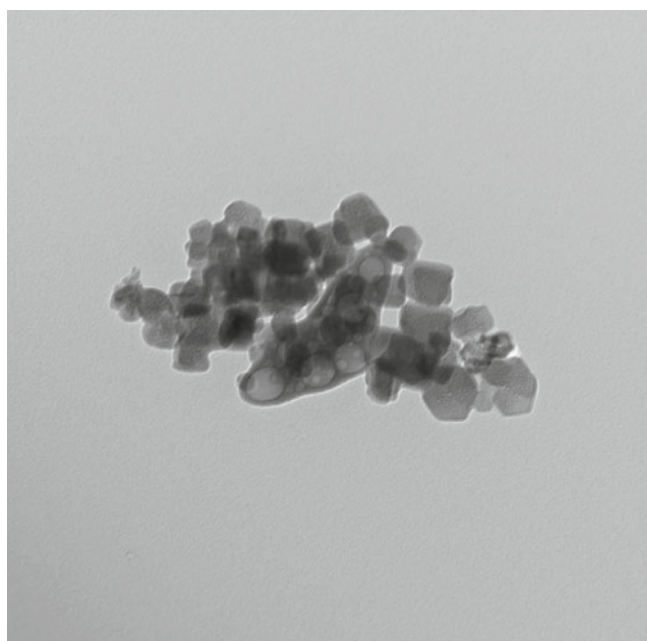


Figure 1. FT-IR spectra of (a) Nujol, (b) $\text{CoCd}_{0.2}\text{Fe}_{1.8}\text{O}_4$, (c) $\text{CoCd}_{0.4}\text{Fe}_{1.6}\text{O}_4$ and (d) $\text{CoCd}_{0.6}\text{Fe}_{1.4}\text{O}_4$ annealed at 1000 °C.



100 nm

Figure 2. TEM micrograph of $\text{CoCd}_{0.2}\text{Fe}_{1.8}\text{O}_4$ annealed at 1000 °C.

resulted during annealing from the driving force provided by the net decrease in the solid–solid and the solid–vapour interface free energy. Most of the ferrite particles have a spherical morphology with an average size of ~ 25 nm.

3.3 X-ray diffraction studies

X-ray diffraction (XRD) patterns of all the as obtained as well as annealed ferrite samples have been recorded. XRD patterns of the as-obtained samples do not show any peak, indicating the amorphous nature of the particles. However,

peaks were observed in the XRD patterns of the samples obtained after annealing at various temperatures for 2 h. XRD patterns of all the compositions annealed at 1000 °C for 2 h are shown in figure 3. They reveal that all the compositions except CoCdFeO_4 possess single phase cubic spinel structure with $Fd\bar{3}m$ space group. In CoCdFeO_4 an extra peak corresponding to Fe_2O_3 phase has been observed. The average crystallite size of all the compositions has been calculated from the line broadening of most intense peak (3 1 1) using the classical Scherrer relationship (Cullity 1976), $D_{hkl} = 0.9\lambda/B\cos\theta$, where D_{hkl} is the particle diameter, B the half-maximum line width, λ the wavelength of the radiation used and θ the angle of diffraction. The average crystallite size is found to be ~ 35 nm (within an error of ± 2 nm) and its values are listed in table 1.

The effect of temperature on the crystallite size has also been studied. Figure 4 shows XRD patterns of $\text{CoCd}_{0.2}\text{Fe}_{1.8}\text{O}_4$ (as obtained as well as those annealed at 400, 600, 800 and 1000 °C). The absence of any peak in the X-ray diffraction pattern of the as-obtained sample indicates its amorphous nature, as reported in our previous papers (Singhal *et al* 2006a, b; Singhal and Chandra 2007). At 400 °C, the peaks are broad signifying lower crystallite size. As the annealing temperature is increased, the peaks become narrower and sharper attributing to the increase in grain size.

The lattice parameter, a , for each composition has been calculated using Pawley refinement method (built in TOPAS V2.1 of BRUKER AXS) and its values are listed in table 1. It is observed that the lattice parameter of Cd^{2+} substituted cobalt ferrites is greater than that of CoFe_2O_4 . This may be due to the fact that the ionic radius of Cd^{2+} ion (0.84 Å) is larger than that of Fe^{3+} ion (0.67 Å). It is also observed that the lattice parameter of all the Co–Cd ferrites varies in the range of 8.3840 to 8.3847 Å. The effect of annealing temperature on lattice parameter has also been studied. It is observed that the lattice parameter remains nearly constant for the samples annealed at 400, 600 and 800 °C. However,

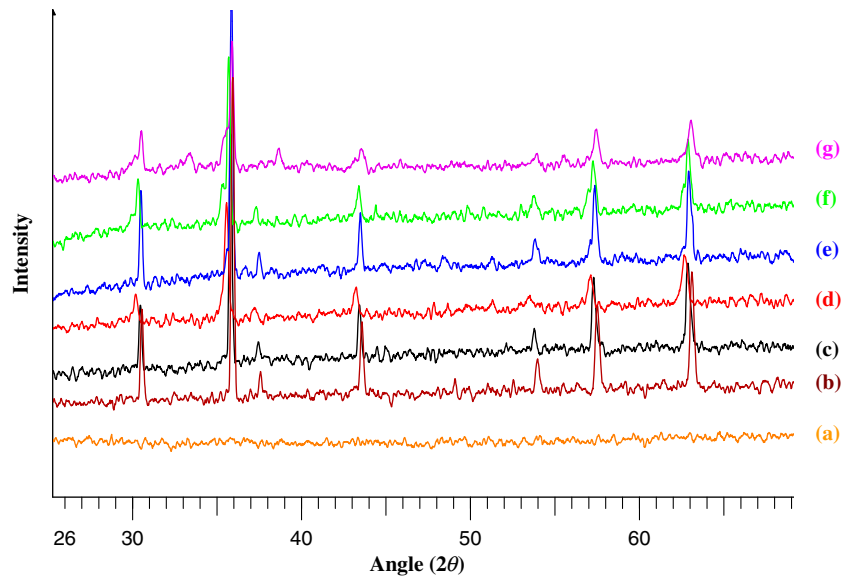


Figure 3. X-ray diffraction (XRD) patterns of (a) $\text{CoCd}_{0.2}\text{Fe}_{1.8}\text{O}_4$ (as obtained) and (b) CoFe_2O_4 , (c) $\text{CoCd}_{0.2}\text{Fe}_{1.8}\text{O}_4$, (d) $\text{CoCd}_{0.4}\text{Fe}_{1.6}\text{O}_4$, (e) $\text{CoCd}_{0.6}\text{Fe}_{1.4}\text{O}_4$, (f) $\text{CoCd}_{0.8}\text{Fe}_{1.2}\text{O}_4$ and (g) CoCdFeO_4 annealed at 1000°C .

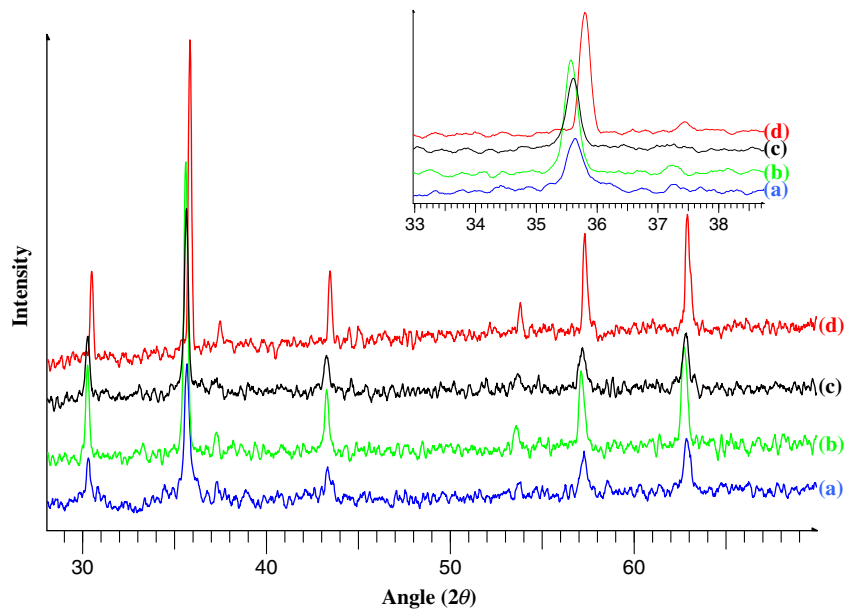


Figure 4. X-ray diffraction (XRD) patterns of $\text{CoCd}_{0.2}\text{Fe}_{1.8}\text{O}_4$ annealed at (a) 400°C , (b) 600°C , (c) 800°C and (d) 1000°C .

Table 1. Lattice parameter, volume of unit cell, crystallite size, saturation magnetization and coercivity of ferrites after annealing at 1000°C .

Ferrites composition	Lattice parameter, $a(\text{\AA})$	Volume (\AA^3)	Crystallite size $D \pm 2$ (nm)	Saturation magnetization, $M_s(\text{emu/g})$	Coercivity, $H_c(\text{Oe})$
CoFe_2O_4	8.3826	589.03	40	84.4	300
$\text{CoCd}_{0.2}\text{Fe}_{1.8}\text{O}_4$	8.3840	589.32	41	73.5	350
$\text{CoCd}_{0.4}\text{Fe}_{1.6}\text{O}_4$	8.3846	589.45	32	75.4	335
$\text{CoCd}_{0.6}\text{Fe}_{1.4}\text{O}_4$	8.3844	589.40	42	67.0	150
$\text{CoCd}_{0.8}\text{Fe}_{1.2}\text{O}_4$	8.3847	589.47	37	45.0	160
CoCdFeO_4	8.3843	589.38	35	49.5	100

the lattice parameter shows a slight decrease for the samples annealed at 1000 °C.

3.4 Magnetic measurements

Typical hysteresis loops for all the as obtained as well as annealed samples have been recorded at room temperature and it has been observed that the saturation magnetization (M_s) increases with increase in annealing temperature. This may be attributed to the increase in the particle size of the ferrites with increase in temperature, as confirmed by the X-ray studies (Morrison and Haneda 1981). The room temperature hysteresis loops of all the ferrite compositions annealed at 1000 °C are represented in figure 5 and the

values of saturation magnetization, M_s and coercivity, H_c , are listed in table 1.

It is observed that the saturation magnetization first increases up to $x = 0.4$ and then it decreases. This may be attributed to the fact that up to $x = 0.4$, the lesser magnetic Cd^{2+} ions occupy the tetrahedral A-sites, which leads to increase in the magnetic moment, in accordance with the Neel's two sublattice model. The substitution of non-magnetic divalent Cd^{2+} ions on the A-sites, transfers the trivalent Fe^{3+} ions to B-sites. But after $x = 0.4$, the magnetization of A-sublattice is so much diluted that the A–B lattice interaction becomes too weak and thereby B–B sublattice interaction becomes strong. This disturbs the parallel arrangements of spins on the B-site and hence canting of

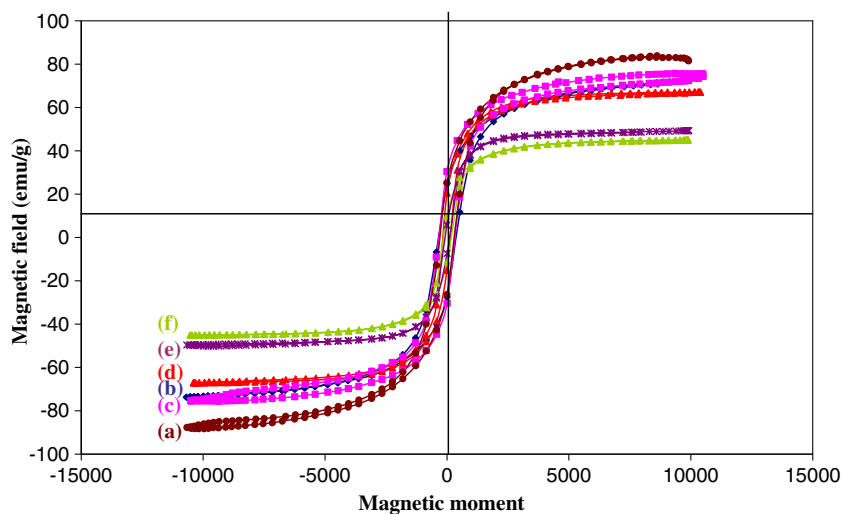


Figure 5. Hysteresis loops of (a) CoFe_2O_4 , (b) $\text{CoCd}_{0.2}\text{Fe}_{1.8}\text{O}_4$, (c) $\text{CoCd}_{0.4}\text{Fe}_{1.6}\text{O}_4$, (d) $\text{CoCd}_{0.6}\text{Fe}_{1.4}\text{O}_4$, (e) $\text{CoCd}_{0.8}\text{Fe}_{1.2}\text{O}_4$ and (f) CoCdFeO_4 annealed at 1000 °C.

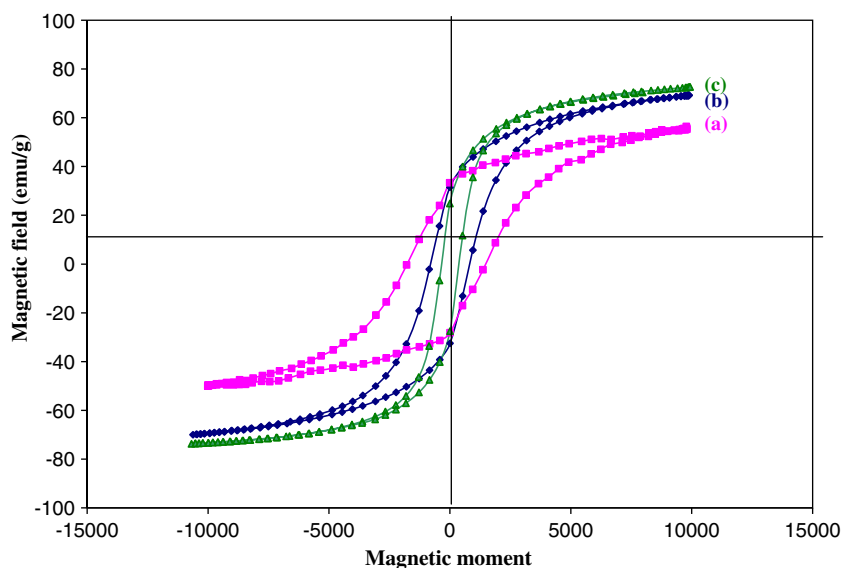


Figure 6. Hysteresis loops of $\text{CoCd}_{0.2}\text{Fe}_{1.8}\text{O}_4$ annealed at (a) 400 °C, (b) 600 °C and (c) 1000 °C.

spin occurs. This gives rise to Yafet–Kittel (Y–K) angle, due to which the saturation magnetization decreases (Yafet and Kittel 1952). This is in accordance with the results reported by other researchers (Akhter and Hakim 2010; Anjum et al 2011). The coercivity is observed to decrease with increase in Cd^{2+} concentration due to decrease in magnetocrystalline anisotropy, which in turn decreases the domain wall energy (Yakovlev et al 1969; Gul et al 2007).

The effect of particle size on the magnetic properties has also been studied. Figure 6 shows room temperature hysteresis loops of $\text{CoCd}_{0.2}\text{Fe}_{1.8}\text{O}_4$ annealed at 400, 600 and 1000 °C. It is observed that as the annealing temperature increases, the saturation magnetization also increases due to increase in particle size.

3.5 Electrical properties

The electrical properties of the ferrite materials are tunable as they depend on the chemical composition, method of preparation, annealing temperature, etc. Properties like electrical conductivity give valuable information about conduction mechanism. The conduction mechanism in ferrites can be explained on the basis of Verwey mechanism (Ashiq et al 2010), involving electron exchange between the atoms of same element present in more than one valence state. It is

believed that at 120 K, charge ordering takes place such that valency of one-third of Fe ions occupying the A-sites of the ferrite lattice is unchanged as 3^+ throughout the entire temperature range and the remaining two-third Fe ions in the octahedral B-sites undergo a change to 2^+ state (Seo et al 2003).

The electrical properties of all the ferrite compositions have been studied using two-probe method. The variation of the d.c. electrical resistivity with temperature is shown in figure 7 and its values are listed in table 2. It is observed that in all the ferrite compositions, the resistivity decreases with increase in temperature, indicating their semiconducting nature. The decrease in the d.c. electrical resistivity with temperature may be due to the increase in hopping of charge carriers between Fe^{2+} – Fe^{3+} ions and Co^{3+} – Co^{2+} ions at the octahedral sites, in accordance with the Verwey mechanism (Ashiq et al 2010). It is also observed that the d.c. resistivity increases with increase in Cd^{2+} concentration. This may be explained on the basis of composition of the ferrite. In case of Co–Cd ferrites, Co ions seek to the octahedral sites, Cd ions to the tetrahedral sites and Fe ions to both the octahedral and the tetrahedral sites. The conductivity of the ferrites may be due to the hopping of electron between Fe^{2+} and Fe^{3+} ions and hopping of holes between Co^{2+} and Co^{3+} ions, which gives rise to n -type and p -type conduction, respectively. The

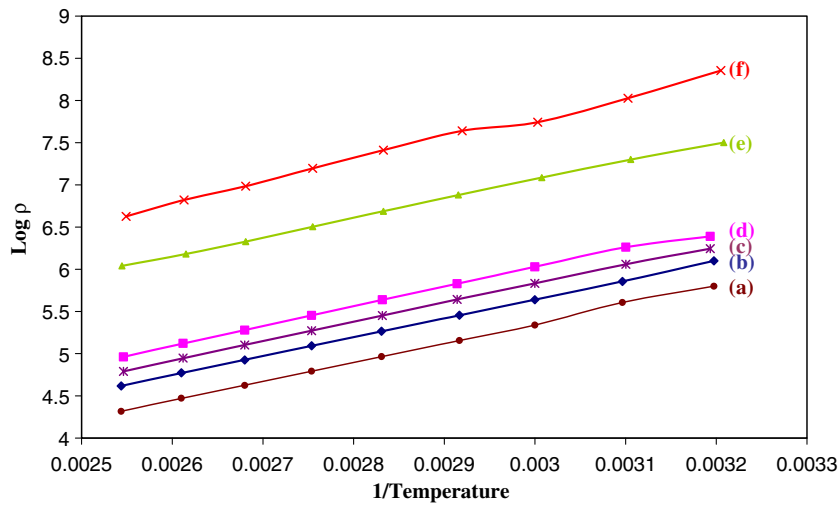


Figure 7. Log ρ vs $1/T$ curves of (a) CoFe_2O_4 , (b) $\text{CoCd}_{0.2}\text{Fe}_{1.8}\text{O}_4$, (c) $\text{CoCd}_{0.4}\text{Fe}_{1.6}\text{O}_4$, (d) $\text{CoCd}_{0.6}\text{Fe}_{1.4}\text{O}_4$, (e) $\text{CoCd}_{0.8}\text{Fe}_{1.2}\text{O}_4$ and (f) CoCdFeO_4 annealed at 1000 °C.

Table 2. D.C. electrical resistivity (ρ), energy of activation (E_a), drift mobility (μ_d) and Seebeck coefficient (S) at 373 K for $\text{CoCd}_x\text{Fe}_{2-x}\text{O}_4$ annealed at 1000 °C.

Electrical property	$x = 0.0$	$x = 0.2$	$x = 0.4$	$x = 0.6$	$x = 0.8$	$x = 1.0$
d.c. Resistivity ($\rho \times 10^7$), $\Omega\text{-cm}$	0.81	0.84	1.38	1.91	1.61	7.26
Activation energy (E_a), eV	0.4471	0.4469	0.4476	0.4479	0.4454	0.5040
Drift mobility ($\mu_d \times 10^{-13}$), $\text{cm}^2 \text{V}^{-1} \text{s}^{-1}$	1090.0	989.6	527.2	317.8	693.9	180.8
Seebeck coefficient (S) μVK^{-1}	137	245	327	703	496	640

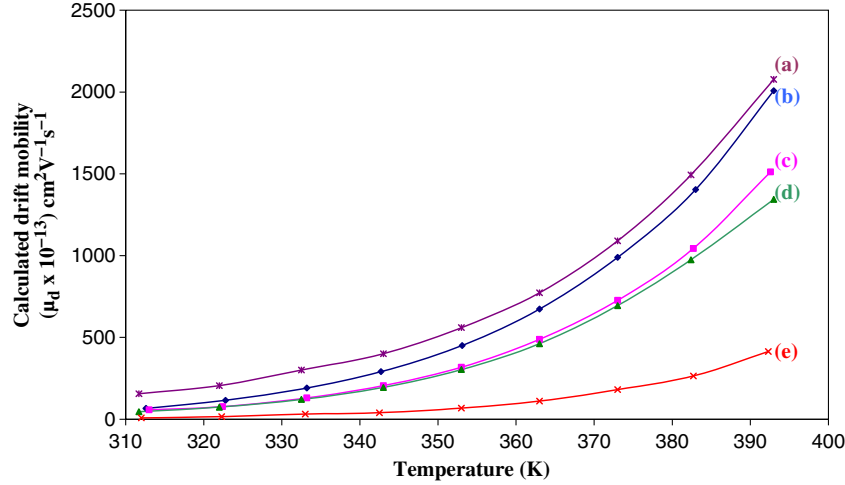


Figure 8. Variation of calculated drift mobility with temperature for (a) CoFe_2O_4 , (b) $\text{CoCd}_{0.2}\text{Fe}_{1.8}\text{O}_4$, (c) $\text{CoCd}_{0.6}\text{Fe}_{1.4}\text{O}_4$, (d) $\text{CoCd}_{0.8}\text{Fe}_{1.2}\text{O}_4$ and (e) CoCdFeO_4 annealed at 1000°C .

replacement of Fe ion by Cd ion leads to decrease in Co ion content in octahedral sites, causing a decrease in the probability of the reaction: $\text{Co}^{2+} + \text{Fe}^{3+} \leftrightarrow \text{Co}^{3+} + \text{Fe}^{2+}$. This causes a decrease in conductivity and a subsequent increase in resistivity. Similar results have been reported by Farea *et al* (2008).

The relationship between the resistivity (ρ) and the temperature may be expressed as $\rho = \rho_0 e^{\Delta E/kT}$, where ρ is the d.c. electrical resistivity, ρ_0 the pre-exponential factor depending on the nature of material, T the absolute temperature, k the Boltzmann constant and ΔE the energy of activation (Carbia-Ruelas *et al* 2011). The values of energy of activation have been calculated from the slope of $\log \rho$ vs $1/T$ graph and are listed in table 2. It is observed that the energy of activation is ~ 0.45 eV.

Drift mobility (μ_d) of the samples has been calculated using the following relation (Barakat *et al* 1991),

$$\mu_d = 1/\eta e \rho,$$

where e is the charge on electron, ρ the resistivity at a particular temperature and η the concentration of charge carriers that can be calculated from the relation (Ajmal *et al* 2010),

$$\eta = (N_A \rho_b P_{\text{Fe}}) / M,$$

where N_A is the Avogadro's number, ρ_b the bulk density of the ferrite samples and P_{Fe} the number of iron atoms in the formula of the oxide. The values of drift mobility for all the ferrite compositions measured at 373 K are listed in table 2. The variation of drift mobility with temperature is shown in figure 8. It can be seen that in all the ferrite compositions, the drift mobility increases with increase in temperature. It may be due to the hopping of charge carriers from one site to another as the temperature increases (Ajmal *et al* 2010). It is also observed that the drift mobility has relatively low value for $x = 1.0$. This may be attributed to the fact that the

resistivity for $x = 1.0$ is very high, which may be due to the presence of Fe_2O_3 phase in it.

The Seebeck coefficient, S , has been calculated using the relation (Ravinder 2000),

$$\eta = N \exp(-Se/k),$$

where η is the concentration of charge carriers, S the Seebeck coefficient, ' k ' the Boltzmann constant, ' e ' the electronic charge and N the density of ferrites. The value of N for ferrites is taken as 10^{22} cm^{-3} . It is observed that all the ferrites have a positive value of Seebeck coefficient indicating p -type conduction. Reddy *et al* (1999) have calculated Seebeck coefficient for zinc substituted cobalt ferrites, $\text{Co}_x\text{Zn}_{1-x}\text{Fe}_2\text{O}_4$ ($0 \leq x \leq 1$), and have reported a large positive value of Seebeck coefficient ($204 \mu\text{V/K}$) for $x = 0.5$.

4. Conclusions

Nano sized ferrites of cadmium substituted cobalt ferrites have been synthesized using sol-gel autocombustion method and the influence of spin canting effect on their structural, magnetic and electrical properties have been studied. Their average crystallite size is found to be ~ 25 nm. The saturation magnetization first increases and then decreases with increase in cadmium substitution. The d.c. electrical resistivity decreases whereas the drift mobility increases with increase in temperature, indicating semiconducting nature of the ferrite samples. The value of Seebeck coefficient is positive establishing p -type semiconducting behaviour.

Acknowledgements

The authors express their grateful thanks to UGC, New Delhi, for providing financial assistance for research work

under scheme of UGC major project; and for providing a fellowship to one of the authors (SJ).

References

- Abdeen A M, Hemeda O M, Assem E E and El-Sehly M M 2002 *J. Magn. Magn. Mater.* **238** 75
- Ajmal M, Shah N A, Maqsood A, Awan M S and Arif M 2010 *J. Alloys Compds* **508** 226
- Akhter S and Hakim M A 2010 *Mater. Chem. Phys.* **120** 399
- Anjum S, Tahir H M, Hussain K, Khaleeq-ur-Rahman M, Rafique M S and Naseem S 2011 *Phys. B: Condensed Matter* **406** 2555
- Ashiq M N, Bibi N and Malana M A 2010 *J. Alloys Compds* **490** 594
- Barakat M M, Henaish M A, Olofa S A and Twafik A 1991 *J. Therm. Anal.* **37** 241
- Carbia-Ruelas E, Sánchez-Vergara M E, García-Montalvo V, Morales-Saavedra O G and Álvarez-Bada J R 2011 *Appl. Surf. Sci.* **257** 3313
- Cedeño-Mattei Y and Perales-Pérez O 2009 *Microelectronics J.* **40** 673
- Chandradass J, Balasubramanian M and Kim K H 2010 *Mater. Manuf. Process* **25** 1449
- Cullity B D 1976 *Elements of X-ray diffraction* (Addison-Wesley Publishing Co. Inc.) Ch. 14
- Deraz N M and Hessien M M 2009 *J. Alloys Compds* **475** 832
- Farea A M M, Kumar S, Batoo K M, Yousef A and Alimuiddin 2008 *Physica B* **403** 684
- Gul I H, Abbasi A Z, Amin F, Anis-ur-Rehman M and Maqsood A 2007 *J. Magn. Magn. Mater.* **311** 494
- Morrison A H and Haneda K 1981 *J. Appl. Phys.* **52** 2496
- Prasad M S R, Prasad B B V S V, Rajesh B, Rao K H and Ramesh K V 2011 *J. Magn. Magn. Mater.* **323** 2115
- Rai R, Verma K, Sharma S, Nair S S, Valente M A, Kholkin A L and Sobolev N A 2011 *J. Alloys Compds* **509** 7585
- Ravinder D 2000 *Mater. Lett.* **44** 130
- Ravinder D, Srinivasa Rao S and Shalini P 2003 *Mater. Lett.* **57** 4040
- Reddy A V R, Mohan G R, Boyanov B S and Ravinder D 1999 *Mater. Lett.* **39** 153
- Seo H, Ogata M and Fukuyama H 2003 *Physica B* **329–333** 932
- Shelar M B, Jadhav P A, Chougule S S, Mallapur M M and Chougule B K 2009 *J. Alloys Compds* **476** 760
- Shelar M B, Jadhav P A, Patil D R, Chougule B K and Vijaya Puri 2010 *J. Magn. Magn. Mater.* **322** 3355
- Singhal S and Chandra K 2007 *J. Solid State Chem.* **180** 296
- Singhal S, Barthwal S K and Chandra K 2006a *J. Magn. Magn. Mater.* **296** 94
- Singhal S, Barthwal S K and Chandra K 2006b *J. Magn. Magn. Mater.* **306** 233
- Waldron R D 1955 *Phys. Rev.* **99** 1727
- Yafet Y and Kittel C 1952 *Phys. Rev.* **87** 239
- Yakovlev Y M, Rubalikaya E V and Lapovok N 1969 *Sov. Phys. Solid State* **10** 2301